Turbulent structures in the flow through compound meandering channels

I. Moncho-Esteve & G. Palau-Salvador
Department of Rural Engineering, Universidad Politécnica de Valencia, Valencia, Spain

K. Shiono
Department of Civil Building Engineering, Loughborough University, Loughborough, United Kingdom

Y. Muto
Shirahama Oceanographic Observatory, DPRI, Kyoto University, Kyoto, Japan.

ABSTRACT: A deep understanding of the turbulent structures associated with the flow through compound meandering channels is of immense interest to river engineers for the creation of flood retention activities. In this study, the turbulent flow structures in a compound meandering channel is simulated by Large Eddy Simulations (LES) using the experimental configuration of Muto and Shiono (1998). Muto and Shiono measured longitudinal, lateral and vertical velocities as well as turbulence intensities at several cross sections along the meandering channel for overbank flow and the data are used for the validation of the simulations. The Large Eddy Simulation is performed with the in-house code LESOCC2. The Reynolds number based on the channel depth h and the bulk velocity u_b is approximately $R_{eh} \approx 6600$. The interaction between the main channel flow and the floodplain flow generates a complicated flow structure which includes several turbulent flow features around the junction between the main channel and the flood plain. LES is used to predict these features. The predicted streamwise velocities and secondary current vectors as well as turbulent intensity are in good agreement with the LDA measurements. In this paper the mean flow field is analyzed and further insight into the complex nature of flow in compound meandering channels is provided based on Large Eddy Simulation.

Keywords: Turbulence, Large Eddy Simulation, Meander, Flooding

1 INTRODUCTION

The environment is strongly influences by rivers which form our landscape continuously and are important for the transport of freights as well as waste water. The watercourse of a natural river is characterized by a curvy shape. The curves or meanders consist of an inner bank and an outer-bank and can be seen to a first approximation as being periodic. Meanders are formed when river flow erodes the outer-banks and widens the river channel. Sediments are transported from the outer to the inner-bank through which the shape of a river is changed continuously. The mechanisms associated to the phenomena described above are still a challenge to scientists and engineers and are not fully understood yet. Due to the effort to handle and regulate rivers, e.g. river restoration, navigation, water quality, production of energy, it is of great importance to engineers in understanding the various governing mechanisms, including secondary motions within the meander channel.

In-bank flow in meandering channels is highly three-dimensional and complex exhibiting secondary motions. The phenomenon of secondary motions was first mentioned by Boussinesq (1868) and Thomson (1876). They studied the center-region cell and discussed the influence of secondary motion on the streamwise velocity distribution and on the sediment transport. Secondary motion occurs due to the imbalance between the driving centrifugal force and the transverse pressure gradient (Jia et al., 2001).

Moreover, river flows in a compound channel often inundate the adjacent plains, which generate more complicated flow structures between the main and the floodplain flows. Compared with the extensive knowledge for straight compound channel flows, much less information is available for compound meandering channel flows. Only some works are available in the literature (Muto & Shiono (1998); Jing et al (2009); Rameshwaran & Naden (2004); Peter R. Wormleaton & Manaye Ewunetu (2006); Rameshwaran & Shiono (2003)). Of special interest is the work by M. Sanjou &

I.Nezu (2006) where a LES simulation has been carried out to study the turbulent flow structures in a meander compound channel with a sinuosity of 1.09 for the meander bend.

The main objective of this project is to complement the experiments in studying the effect of the interaction between the main channel flow and the floodplain flow on the mean and instantaneous flow, the turbulent and related structures as well as the distribution of mean and instantaneous bed-shear stresses. However, in this paper only the comparison of the mean velocities and the turbulent intensity are discussed.

2 EXPERIMENTAL SET-UP

The experiment was carried out at the hydraulics laboratory, Department of Civil and Environmental Engineering, University of Bradford. The experimental flume consisted of 5 meanders, where the bends were connected by straight sections (see Figure 1). It was made of Perspex with a rectangular cross-section.

The flume was equipped with a recirculation pump-sump system and a venturimeter pipe was installed in the middle of the recirculation system, to which a hybrid trans-former-oil/mercury manometer was detached for discharge measurement. The calibration curves relating manometer readings and discharge were obtained by Alromaih (1996) beforehand.

The velocity measurement was carried out with 2 component laser-Doppler anemo-meter (LDA) and flow visualization at the water surface using solid tracers and a fixed camera technique.

The longitudinal slope (valley slope) of the flume was adjustable with a jack and a hinge. The slope was reestablished after installing each new configuration of meander channel and was checked with a dial gauge frequently during the experiments.

The central radius of channel curvature r_c was 0.425 m and the arc of meander was 120° with the corresponding sinuosity 1.370. The width of the channel was 0.15 m and the depth 0.053 m. More details of the case are specified in table 1.

3 NUMERICAL METHOD

The LES was performed with the in-house code LESOCC2 (Large Eddy Simulation On Curvilinear Coordinates). It is a successor of the code LESOCC developed by Breuer and Rodi (1996). The code solves the Navier-Stokes equations on body-fitted, curvilinear grids using a cell-centered finite volume method with collocated storage arrangement. Second-order central differences are employed for the convection as well as for the diffusive terms. The time integration is performed with a predictor-corrector scheme, where the explicit predictor step for the momentum equations is a low-storage three-step Runge-Kutta method. The corrector step covers the implicit solution of the Poisson equation for the pressure correction. The subgrid-scale (SGS) stresses, resulting from the unresolved motions, are modelled using the approach of Smagorinsky (1963) with a model parameter of $C_s=0.1$.

For the numerical calculation a global coordinate system was used, while for the data analysis the quantities were transformed on a body-fitted coordinate system. The x-axis is hereby along the centerline of the channel bed, the y-axis is along the spanwise direction and the z-axis is along the vertical direction. The Reynolds number based on the bulk-velocity and the hydraulic radius is 6600. The cross-sectional aspect ratio of channel width to water depth is 2.5 and the flood plain depth is 0.01 m. The computational grid consists of $960 \times 90 \times 40 = 3.456 \cdot 10^6$ grid points in the in-bank and $960 \times 390 \times 10 = 3.744 \cdot 10^6$ in the outer-bank in the x-, y- and z-directions, respectively. The characteristic of the mesh in a cross section of the compound meander is shown in Figure 1.

The computational grid is uniform along the centerline in x-direction and stretched in the y- and z-directions to achieve a better resolution of the near wall motions. The stretching ratio is kept to a fix value around 1.03. The grid sizes in terms of wall units are $\Delta y^+ = \Delta z^+ \approx 17$ near the wall and $\Delta x^+ \approx 200$. Only one meander was computed and periodic boundary conditions were defined in the entrance and exit of the meander. The Werner-Wengle model was employed at the bottom boundary and lateral walls jointly with a rigid-lid assumption for the free surface.

4 RESULTS & DISCUSSION

In this section, some results of the simulation are presented. Focus is given to the mechanism of secondary motion and the importance of the mean velocity and the turbulent intensity is also highlighted in the discussion.

4.1 *Mean flow*

The comparison of the mean streamwise velocity contour lines between the LES simulation and the experimental data by Muto (1997) is presented in Figure 2. In the figure, the distances of the lateral and vertical components are normalized by the channel height and the mean velocity by the
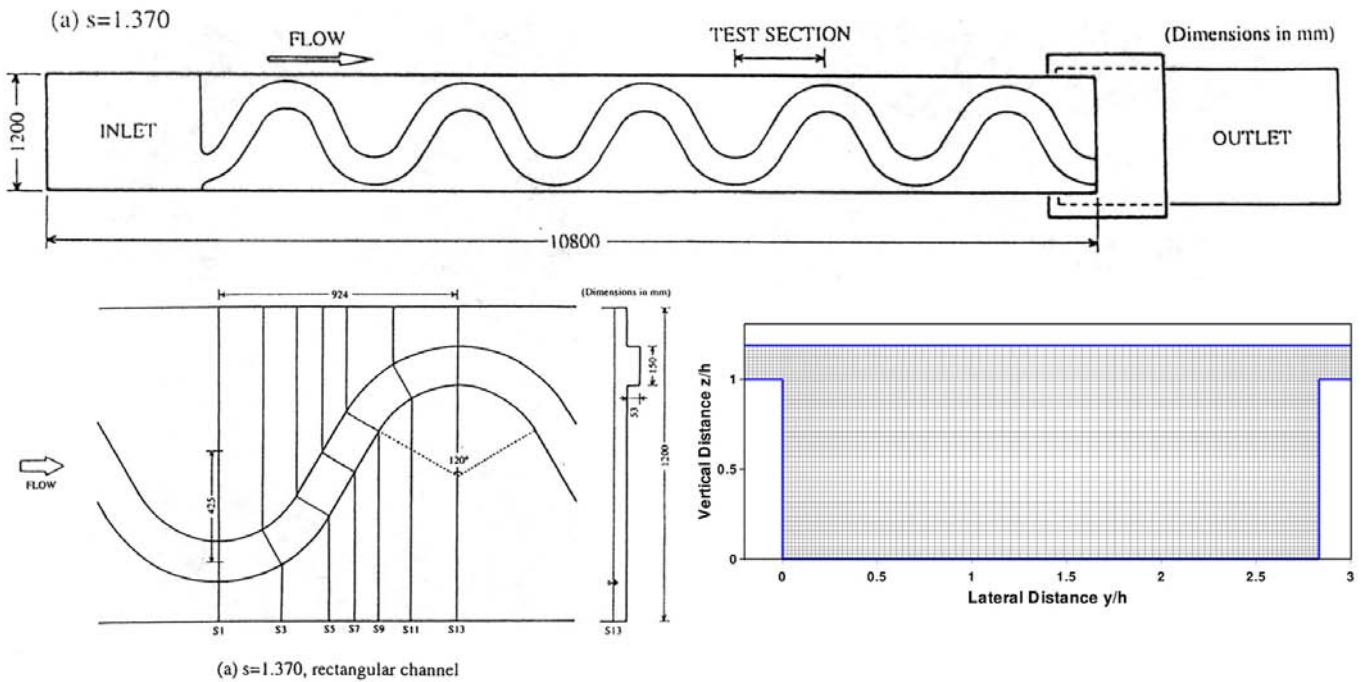
Figure 1. Experimental set-up and detail of the mesh used in the LES simulation

Table 1 Meandering channel of the experiments of Muto (1997)

Discharge	Water Depth	Relative depth	Mean velocity	Friction velocity[a]	Reynolds number[b]	Froude number[c]
Q ($\cdot 10^{-3}$m^3/s)	H (m)	(H-h)/H	U_s (m/s)	u_* (m/s)	Re ($\cdot 10^3$)	Fr
2.513	0.063	0.15	0.129	0.012	6.6	0.34

a. $u_* = \sqrt{gRS}$, where g=gravity acceleration, R=hydraulic radius and S=energy slope

b. Re=4U_sR/ν, where ν=kinematic viscosity, R=hydraulic radius

c. Fr=U_s /(gR)$^{-1/2}$

section averaged velocity (U_s=Q/A; where Q is the discharge and A is the cross area).

The LES results show a very good agreement with the experimental results by Muto (1997), in particular for the prediction of the maximum values. In this case, the flow behaviour is different to what happens in the case of the in-bank flow for meander channel. The maximum velocity values occur near both channel walls at the bend apex and lower velocities occur in the central region. This is well related with the structure of the secondary flow motions explained in the next section.

Moreover, in the crossover region (sections 5-9), it also appears a clear influence of the flood-plain flow to a vertical gradient of the velocity contour lines due to the floodplain flow entering this region. There are some discrepancies between the computed and measured velocity patterns near water surface in the cross-over sections in which water level varies along the cross–over sections due to entering floodplain flow. This can be expected owing to the use of rigid lid condition in the computation. However, the streamwise motion

is still dominant in the major domain with values higher than the section mean velocity U_s.

4.2 *Secondary currents*

To analyze in detail the secondary currents in the compound meandering channel, the secondary current vectors of the selected sections are presented in Figure 3 and compared with the experimental results by Muto (1997).

For the in-bank flow case, the process of the growth and decay of the primary vortex has already been analyzed in Folke et al. (2009). However, the effect of the floodplain flow complicates the behavior in this case (Figure 3). In section 1, a big anti-clockwise recirculation cell could be observed in the vicinity of the inner bend. However, this dissipates along the next reach by entering floodplain flow which produces two smaller cells near the inner wall in section 3, although this is not clearly seen in the experimental result. Moreover, at section 5 a new cell appears around y/h=0.8 which starts progressing downstream to situate the inner wall. This cell could be the upper

cell grown by the floodplain flow near the inner wall at section 3. Surprisingly, the progress of the primary vortex generated by the floodplain flow along the meandering channel is well predicted. In future analysis, the location and generation of this primary vortex will be analyzed.

4.3 *Turbulent intensity*

The turbulent intensity is analyzed by the value of the root-mean-square (rms) of streamwise velocity fluctuations normalized by the friction velocity (u_*) and presented in Figure 4. At this moment, fluctuations were recorded during 500 dimensionless time units H/U_∞.

The results show a good agreement with the experimental results by Muto (1997) except near water surface areas. Maximum values are around 2.25 and they appear in shear layer regions where the flow interaction occurs by the floodplain flow entering main channel in the upper left corner of sections 5-9. This interaction is also well reproduced by LES.

5 CONCLUDING REMARKS

In this paper, the results of a large eddy simulation of the flow in a periodic compound meandering channel for overbank flow were presented. The comparison with experimental data of the streamwise velocity and secondary currents in selected cross sections was made and was satisfactory.

Our main interest concerns the development of the secondary motions and their possible implications for sediment transport, meander formation and stabilization. We have shown that, for this particular depth case, one interacting cell after the bend apex is formed that switches from one bend to the other, but opposite to what happens in the in-bank flow case. After the switch from bend apex to apex it is dissipated by the water intrusion from the floodplain, on the other hand a new cell emerges. In spite of the (low?) strength of this recirculation cell, they are very relevant to turbulent transport and mixing along the meandering channel.

REFERENCES

Boussinesq, J. (1868). Mémoire sur l'influence des frottements dans les mouvements reguliers des fluids. J. Math. Pures Appl. (2me sér.), 13, 377-424.

Breuer, M. & Rodi, W. (1996). Large eddy simulation of turbulent flow through a straight square duct and a 180° bed. Fluid Mechanics and its Applications, 26, 273-285.

Folke, F., Moncho-Esteve I.J., García-Villalba, M., Braun, C. & Palau-Salvador, G. (2009). Large eddy simulation of flow in meandering open channels. 33rd International Association of Hydraulic Engineering & Research (IAHR) Biennial Congress, Vancouver, 9-14 August.

Jia, Y., Blanckaert, K. & Wang, S.S. (2001). Numerical simulation of secondary currents in curved channels. Proc. 8th FMTM-congress, Tokyo.

Jing, H., Guo, Y., Li, C., & Zhang, J. (2009). Three-dimensional numerical simulation of compound meandering open channel flow by the Reynolds stress model. International Journal for Numerical Methods in Fluids, 59, 927-943.

Muto, Y. (1997). Turbulent Flow in Two-Stage Meandering Channels. Ph.D. thesis, University of Bradford, UK.

Rameshwaran, P. & Naden P. (2004). Modelling turbulent flow in two-stage meandering channels. Proceedins of the Institution of Civil Engineers-Water Management, 157(3), 159-173.

Rameshwaran, P. & Shiono, K. (2003). Computer modeling of two-stage meandering channel flows. Proceedins of the Institution of Civil Engineers-Water & Maritime Engineering, 156(4), 325-339.

Shiono, K. & Muto, Y. (1998). Complex flow mechanism in compound meandering channels with overbank flow. J. Fluid Mech., Cambridge Univ. Press, 376, 221-261.

Sanjou, M & Nezu, I. (2006). Large eddy simulation of turbulent structure in meandering compound open-channel flow. River Flow 2006, Vol 1-2, 253-260.

Wormleaton, P. R. & Ewunetu M. (2006). Three-dimensional k-e numerical modeling of overbank flow in a mobile bed meandering channel with floodplains of different depth, roughness and planform. Journal of Hydraulic Research, 44(1), 18-32.
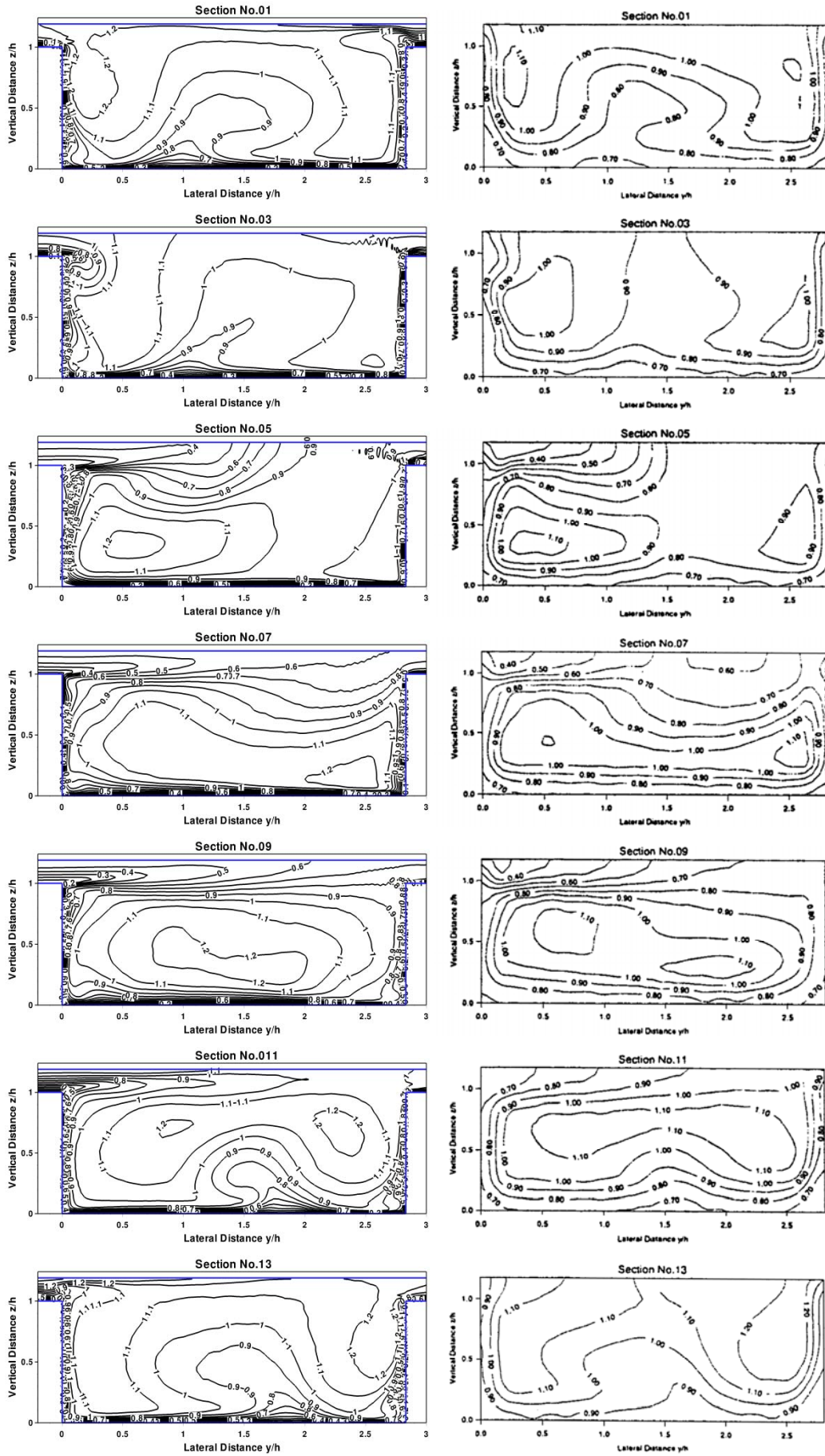
Figure 2. Streamwise velocity U/U$_s$ (Left: LES simulation; Right: experimental measurements by Muto (1997))
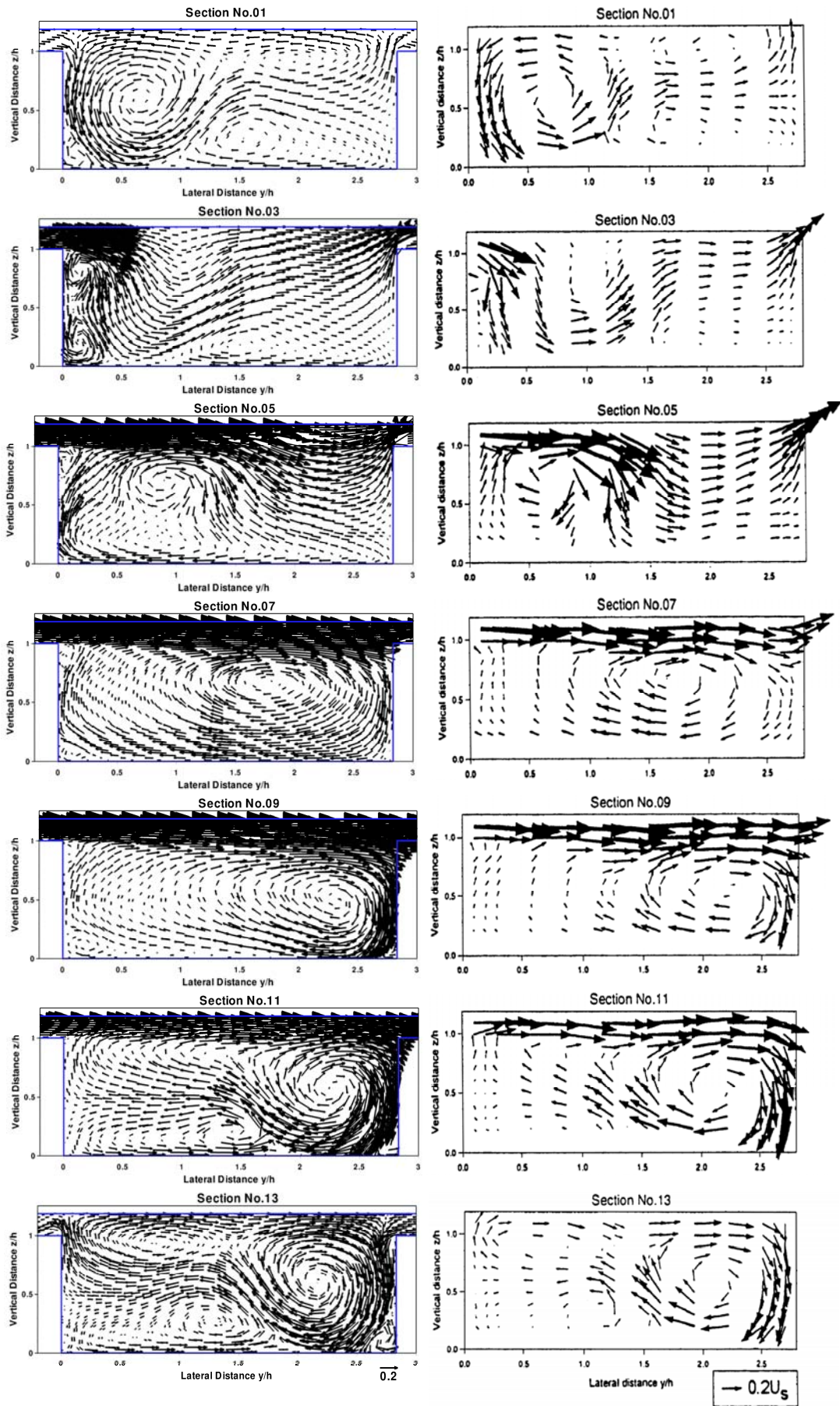
Figure 3. Secondary flow vectors (Left: LES simulation; Right: experimental measurements by Muto (1997))
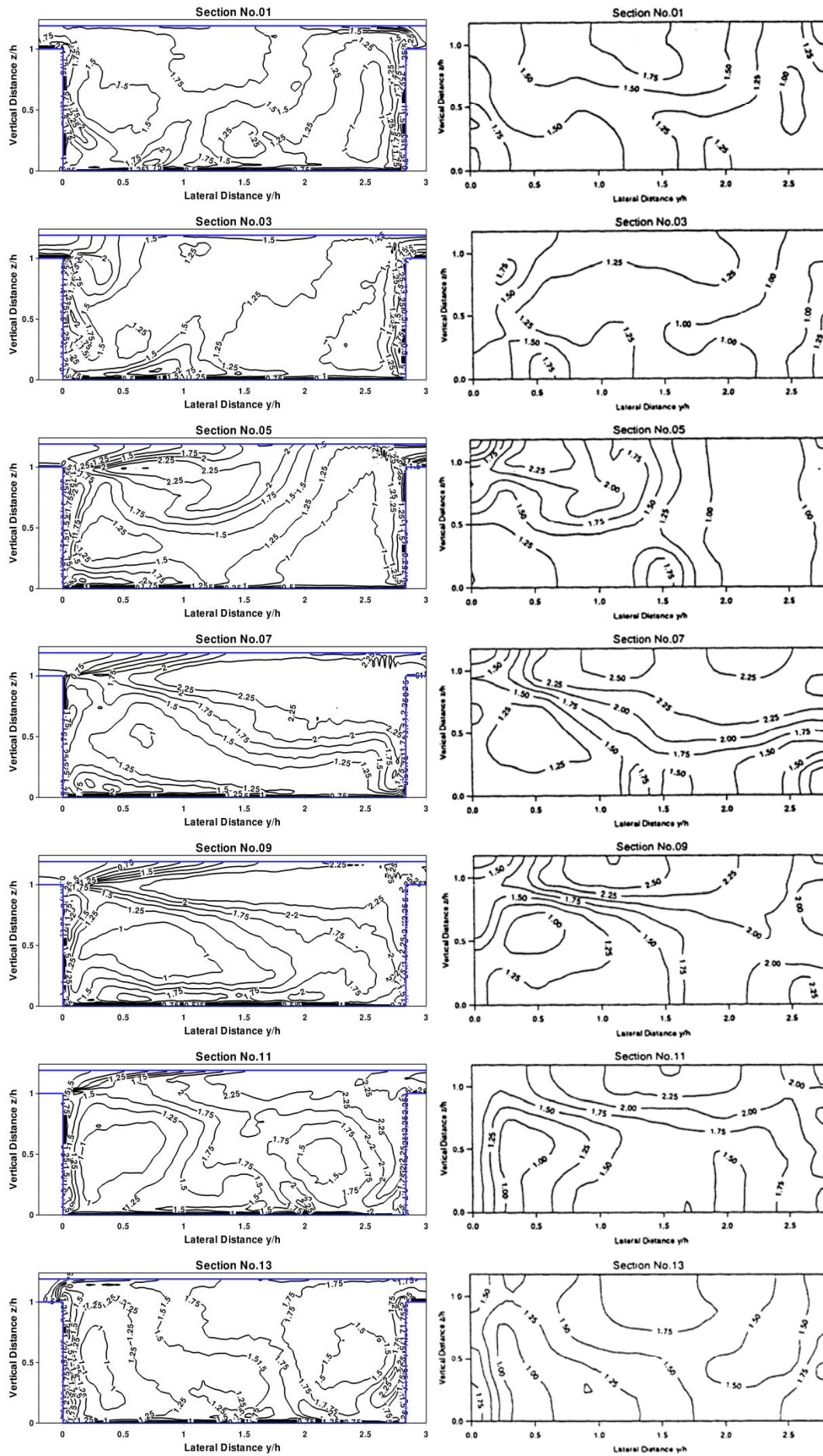
Figure 4. Turbulent intensity u´/u∗ (Left: LES simulation; Right: experimental measurements by Muto (1997))